Turbulence of Non-orographic Gravity Waves in Mars Planetary Climate Model.

Jiandong Liu[1,2], **Ehouarn Millour**[1], **Francois Forget**[1], **Francois Lott**[1], [1]*LMD/IPSL, Sorbonne Université, ENS, Université PSL, École Polytechnique, Institut Polytechnique de Paris, CNRS, Paris, France (jiandong.liu@lmd.ipsl.fr)*, [2]*Laboratoire de Physique et Chimie de l'Environnement et de l'Espace, CNRS/Université d'Orléans, UMR 7328, Orléans, 45071, France*, **Jean-Yves Chaufray**, *LATMOS, CNRS, Sorbonne Université, Université Versailles St-Quentin, Paris, France*.

Introduction

The dynamics of Mars' upper atmosphere play a key role in controlling the transport and escape of atmospheric gases. These processes are crucial for understanding how Mars' atmosphere has evolved over time and what that means for the planet's past habitability[1,2]. Measurements of neutral species in the upper atmosphere have revealed unexpected fluctuations in density[3,4,5]. These variations cannot be fully explained by current model simulations, even when both internal and external forcings are carefully included[3,4]. Orographic gravity waves generally have limited influence above the middle atmosphere[6]. As a result, recent research has shifted toward understanding the impact of non-orographic gravity waves[3,7,8,9]. Turbulence generated by these waves is now considered a likely cause of the observed variability in upper atmospheric densities[2,3,4,5].

We introduce a new way to model mixing caused by non-orographic gravity waves in the Mars Planetary Climate Model. This approach links wave propagation and turbulence using the same set of assumptions, forming a unified framework. It gives a surface-to-exosphere parameterization of mixing through an eddy diffusion coefficient. Simulations show that the coefficient ranges from 10^4 to 10^9 cm^2 s^{-1}. The turbopause lies between 70 and 140 km, depending on the season. While temperatures change only slightly, the mixing strongly affects the distribution of tracers in the upper atmosphere. Results agree well with data from Mars Climate Sounder and NGIMS. This scheme shows how gravity wave-driven turbulence can boost vertical transport and help control upper atmospheric processes like tracer escape.

Methodologies and Assumptions

Early studies proposed that turbulence in the upper atmosphere can result from localized unstable layers created by gravity wave saturation[7]. Once turbulence is triggered in these regions, it acts to suppress further instability. This idea was later formalized by assuming that turbulence fully eliminates instability in thin layers around the wave saturation levella concept we refer to as the **Non-Superadiabatic Principle** (NSP).

The NSP has been useful in linking turbulence generation to wave saturation, but it has limitations. Specifically, it may overestimate turbulence above the saturation level and fails to fully account for turbulence observed below it.

We revisit the NSP without changing the original formalism, but with a more constrained interpretation based on four key points:

(a) Turbulence is generated by instabilities arising from the wave's momentum deposition into the mean flow, as seen in temperature fluctuations. This implies that eddy diffusivity is proportional to the divergence of wave momentum.

(b) As a result, turbulence should occur both above and below the saturation level, maintaining vertical symmetry.

(c) The turbulence acts to suppress further instability, preventing excessive temperature gradients from forming during wave momentum deposition.

(d) The maximum turbulence occurs at the saturation level, where the momentum transfer from the wave to the mean flow is strongest.

Additionally, the impact of gravity wave-induced eddy diffusion is typically represented as a **linear damping** process starting at the wave saturation level and extending upward[7]. This approach treats diffusion as a form of dissipation that affects both the energy and momentum of the mean flow[7,8].

Formalism and Results

The governing equations under the assumptions of shallow, inviscid, adiabatic, non-rotating, steady, hydrostatic, incompressible atmosphere may be linearized as,

$$\xi = \underbrace{\bar{\xi}}_{mean} + \underbrace{\xi'}_{pertubation} \tag{1}$$

$\forall \xi \in [u, v, w, \rho, \theta, T, p]$. The wave solution to the perturbation ξ' in (1) may be written as,

$$\xi' = \underbrace{\hat{\xi}}_{amplitudes} e^{i(kx+ly+mz-\omega t)} \tag{2}$$

The governing equations in amplitude $\hat{\xi}$ form (i.e., polarized equations) can be used to derive the Taylor-Goldstein (TG) equation. The solution $\hat{\xi}$ of TG is used to describe the wave.

The Taylor-Goldstein equation in the wave amplitude space $\hat{\xi}$ presents as follows[3,7,8],

$$\frac{d^2}{dz^2}\hat{\xi}+\frac{1}{\bar{\rho}}\frac{d\bar{\rho}}{dz}\frac{d}{dz}\hat{\xi}+\left(\frac{\vec{k}^{[2]}N^2}{\Omega^2}+\frac{\vec{k}\bar{u}_{zz}}{\Omega}+\frac{\vec{k}}{\Omega}\frac{1}{\bar{\rho}}\frac{d\bar{\rho}}{dz}u_z-\vec{k}^{[2]}\right)\hat{\xi}=0 \tag{3}$$

Here $\hat{w}=ik\hat{\xi}$ represents the amplitude of gravity wave; $i^2=-1$; $\vec{k}=(k,l)$ is the horizontal wavenumber; $\vec{k}^{[2]}:=(k^2,l^2)$; z for altitude; $\bar{\rho}$ the background density; N^2 for Brunt-Väisälä frequency; $\Omega=\vec{k}(\vec{k}/(k,l)c-(\bar{u},\bar{v}))$ is the intrinsic frequency with Doppler shift, with c the phase speed and $\bar{u}$ ($\bar{v}$) background zonal (meridional) velocity.

Amusing the background density $\bar{\rho}=\bar{\rho}_r\exp(-z/H)$, the second term of the right side of equation (3) may be eliminated by giving $\hat{w}$ a factor $e^{z/2H}$, i.e., $\hat{w}e^{z/2H}$. The vertical wavenumber $m_r^2=\vec{k}^{[2]}N^2/\Omega^2$ dominates the terms inside the bracket of equation (3). The perturbations w_j' for a monochromatic wave j in (2) yields,

$$w_j'=\hat{w}_j(z)\underbrace{e^{z/2H}}_{\rho(z)}e^{i(k_jx+l_jy+m_jz-\omega_jt)} \tag{4}$$

The gravity waves are naturally stochastic. In practice, we parameterize these waves using wave ensembles ($w'=\sum_{j=1}^{M}C_jw_j'$) that include a few or tens of monochromatic harmonics with random wavenumbers, phase velocities, and momenta.

The approximation solution to (3) for a slowly varying m^2 is termed WKB approximation,

$$\hat{w}(z)\approx A(z)|m_r|^{-1/2}exp\left(i\int_0^z md\zeta\right) \tag{5}$$

It is also written in an iteration form one layer (ll) to another ($ll+1$),

$$\hat{w}_j(z_{ll+1})=\hat{w}_j(z_{ll})\sqrt{\frac{m_r(z_{ll})}{m_r(z_{ll+1})}}exp\left(i\int_{z_{ll}}^{z_{ll+1}}m^{ave}d\zeta\right) \tag{6}$$

By considering **critical layers**, **viscosity damping**, (gravity wave induced) **turbulence damping**, and **saturation**, the wave amplitude $\hat{w}$ reads,

$$\hat{w}_j(z_{ll+1})=\underbrace{\Theta[\Omega(z_{ll+1})\Omega(z_{ll})]}_{\textbf{CL}}\times$$
$$\textbf{MIN}\left\{\hat{w}_j(z_{ll})\sqrt{\frac{m(z_{ll})}{m(z_{ll+1})}}\exp\left(-\underbrace{\frac{\mu*}{\rho}}_{\textbf{VD}}\overbrace{\frac{m_r^3}{\Omega}}^{\textbf{TD}}\delta z\right),\underbrace{\hat{w}_{j,s}}_{\textbf{ST}}\right\} \tag{7}$$

where $\mu*=\mu\bar{D}^j_{eddy}$, $\bar{D}^j_{eddy}$ is the averaged eddy diffusion coefficient. The wave EP-flux is defined as [3,8,9],

$$\vec{E}_j^{z_r}(k_j,l_j,\omega_j)=-\rho_r\frac{\vec{k}}{2\vec{k}^{[2]}}m_j(z_r)|\hat{w}_j(z_r)|^2 \tag{8}$$

Inserting (7) to (8), yields,

$$\vec{E}_j^{z_{ll+1}}=\frac{\vec{k}\Omega}{|\vec{k}||\Omega|}\Theta[\Omega(z_{ll+1})\Omega(z_{ll})]\times$$
$$\textbf{MIN}\left\{|\vec{E}_j^{z_{ll}}|e^{-2\frac{\mu m^3}{\rho\Omega}\delta z},\rho_rS_c^2e^{-\frac{z_{ave}}{H}}\frac{|\Omega|^3k^{*2}}{2N|\vec{k}|^4}\right\} \tag{9}$$

The divergence of the EP-flux of the ensemble is added to the mean flow in terms of the first-order Auto Regression algorithm (AR-1),

$$\left(\frac{\partial\vec{u}}{\partial t}\right)_{GW}^{t+\delta t}=\frac{\delta t}{\Delta t}\frac{1}{M}\sum_{j=1}^{M}\frac{1}{\rho}\frac{d\vec{E}_j}{dz}+\frac{\Delta t-\delta t}{\Delta t}\left(\frac{\partial\vec{u}}{\partial t}\right)_{GW}^{t} \tag{10}$$

The unknown terms in (7) include turbulence damping and saturation. They can be solved by applying NSP to the energy equation. According to the energy equation, the wave-induced vertical temperature gradient follows,

$$\Re\left\{\frac{d\delta T}{dz}\right\}=-\frac{\Gamma A|m_r|^{3/2}e^{\int_0^z(\frac{1}{2H}-m_i)d\zeta}}{N|\vec{k}|},z\in(0,+\infty) \tag{11}$$

At the saturation altitude, the saturated turbulent vertical wavenumber $m_{i,s}$ eliminates the exponential increase of (11), which returns,

$$\frac{1}{2H}+\frac{3}{2}\left|\frac{1}{N}\frac{\partial N}{\partial z}-\frac{1}{\Omega}\frac{\partial\Omega}{\partial z}\right|=m_{i,s},\quad z=z_b,\quad\forall j\in[1,M] \tag{12}$$

Equation (12) implies that the turbulence is at its maximum at z_b, and thus the absolute temperature gradient in (11) is forced to equal the environmental lapse rate Γ. That is,

$$A^2m_r^{-1}\exp\left(-2\int_0^{z_b}m_id\zeta\right)$$
$$=m_r^{-4}N^2|\vec{k}|^2\exp\left(-\int_0^{z_b}\frac{1}{H}d\zeta\right),\quad z=z_b \tag{13}$$

Implementing (13) and (5) into (8) can get the saturated EP-flux in (9, right side inside the bracket).

The turbulence contributes a dissipation term to the momentum and energy equation[7],

$$D^j_{eddy}\frac{\partial}{\partial z^2}\begin{Bmatrix}\hat{\bar{u}}\\ \delta\hat{T}\end{Bmatrix}=-m_r^2D^j_{thermal}\begin{Bmatrix}\hat{\bar{u}}\\ \delta\hat{T}\end{Bmatrix},\quad z\geq z_b \tag{14}$$

Here the Prandtl number equals 1. By the relationship between c_i and m_i, we have,

$$m_i=\frac{N|\vec{k}|m_r^2D^j_{eddy}}{\Omega^2},\quad z\geq z_b \tag{15}$$

The D^j_{eddy} can be derived using (12), (13), (5), (8), and empirical equations[5].

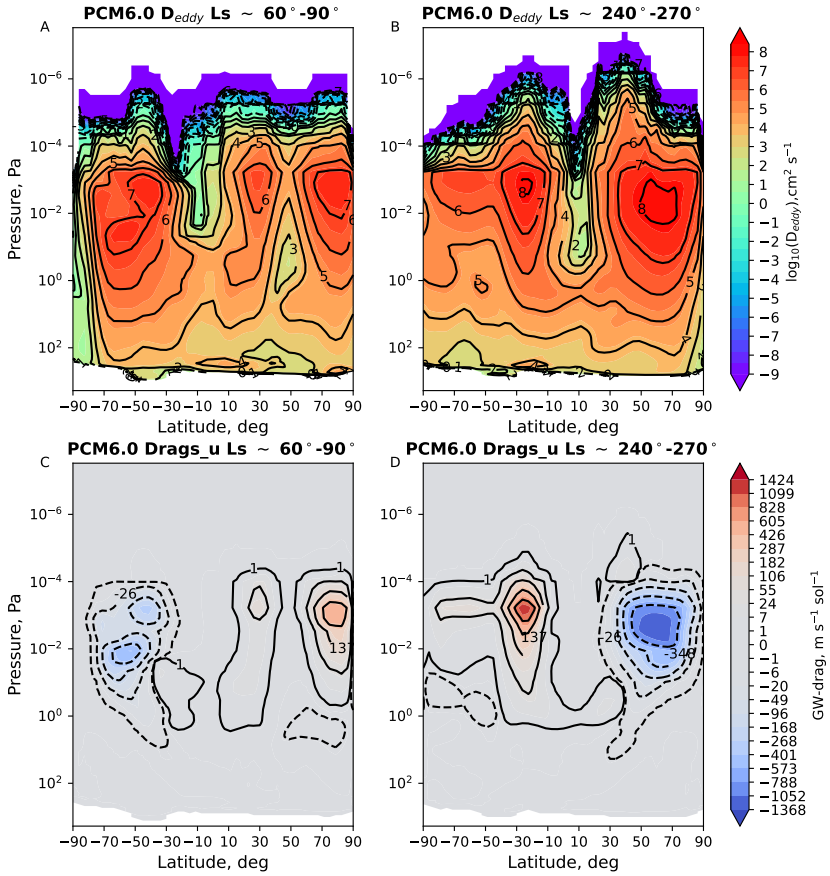

Figure 1: Monthly-averaged zonal averaged D_{eddy} (cm^2 s^{-1}, upper panels) and zonal drags (m s^{-1} sol^{-1}, lower panels) during clear-sky (Ls 60°-90°) and dusty seasons (240°-270°), MY32. Note that the D_{eddy} is plotted in $\log_{10}$ and the contour lines of the drags are nonlinear.

By citing NSP and observations in the lower and middle atmosphere, the eddy coefficient for a given monochromatic wave follows,

$$D^j_{eddy} = \begin{cases} \textbf{MIN}\left[\alpha_{eff}\frac{\Omega}{N^2|\vec{k}|}\left(-\frac{1}{\rho}\frac{\partial \vec{E}}{\partial z}\right), \quad S_{mix}\frac{\Omega^4}{N^3|\vec{k}|^3}\left(\frac{3}{2}\left|\frac{1}{N}\frac{dN}{dz}-\frac{1}{\Omega}\frac{d\Omega}{dz}\right|+\frac{1}{2H}\right)\right] & \text{for} \quad z \geq z_b \\ D^j_{eddy}(z_b)\exp\left[\beta_{diff}\frac{(z-z_b)}{H}\right] & \text{for} \quad z < z_b \end{cases} \tag{16}$$

We use three tunable parameters: the effective mixing factor $\alpha_{eff} = 0.1$, the mixing saturation factor $S_{mix} = 0.1$, and the diffusion decay rate $\beta_{diff} = 1.5$. Equation (16) applies across the saturation altitude z_b, where the eddy diffusivity is set to $D^j_{eddy}(z_b)$. At this level, wave-induced mixing reaches its peak (NSP-d). Above z_b, the mixing decreases with the divergence of wave momentum (NSP-a). Below z_b, it also decreases from the peak value (NSP-a). The divergence of wave momentum above z_b is easy to evaluate, since the Eliassen{Palm (EP) flux is already included in the non-orographic gravity wave (GW) schemes, as shown in Equation (7).

Figure 1 shows the total diffusion coefficient, $\sum_{j=1}^{8} D^j_{eddy}$. Simulations from the Mars PCM indicate that wave-driven momentum can generate eddy diffusion coefficients ranging from 10^6 to 10^7 cm^2 s^{-1} at pressures between 10^0 and 10^{-4} Pa during clear-sky seasons. During dusty seasons, this value increases to 10^7-10^8 cm^2 s^{-1}, and in some cases can reach up to 10^9 cm^2 s^{-1}. This enhancement is linked to stronger wave momentum and higher wave-breaking altitudes. Mars has a variable turbopause, located between 70 and 140 km depending on latitude and season. This highlights the critical role of gravity wave-induced turbulence in atmospheric escape processes.

References

[1] Jakosky, Bruce M., et al. "Mars' atmospheric history derived from upper-atmosphere measurements of 38Ar/36Ar." Science 355.6332 (2017): 1408-1410.

[2] McElroy, Michael B., and Thomas M. Donahue. "Stability of the Martian atmosphere." Science 177.4053 (1972): 986-988.

[3] Liu, Jiandong, et al. "A surface to exosphere non-orographic gravity wave parameterization for the Mars Planetary Climate Model." Journal of Geophysical Research: Planets 128.7 (2023): e2023JE007769.

[4] Slipski, Marek, et al. "Variability of Martian turbopause altitudes." Journal of Geophysical Research: Planets 123.11 (2018): 2939-2957.

[5] Yoshida, Nao, et al. "Variations in vertical CO/CO2 profiles in the Martian mesosphere and lower thermosphere measured by the ExoMars TGO/NOMAD: Implications of variations in eddy diffusion coefficient." Geophysical Research Letters 49.10 (2022): e2022GL098485.

[6] Forget, François, et al. "Improved general circulation models of the Martian atmosphere from the surface to above 80 km." Journal of Geophysical Research: Planets 104.E10 (1999): 24155-24175.

[7] Lindzen, Richard S. "Turbulence and stress owing to gravity wave and tidal breakdown." Journal of Geophysical Research: Oceans 86.C10 (1981): 9707-9714.

[8] Lott, François, Lionel Guez, and P. Maury. "A stochastic parameterization of non-orographic gravity waves: Formalism and impact on the equatorial stratosphere." Geophysical Research Letters 39.6 (2012): L06807

[9] Kling, Alexandre, et al. "Impact of grid resolution on wave-mean flow interactions with high resolution Mars global climate model simulations." Geophysical Research Letters 52.2 (2025): e2024GL112297.